

A Biotin Targeting Chimera (BioTAC) System to Map Small Molecule Interactomes *in situ*

Andrew J. Tao^{*1}, Jiewei Jiang^{*1}, Gillian E. Gadbois¹, Pavitra Goyal¹, Bridget T. Boyle¹, Elizabeth J. Mumby², Samuel A Myers³ Justin G. English^{2,4}, Fleur M. Ferguson^{1,4,5}

¹Department of Chemistry and Biochemistry, University of California San Diego, La Jolla, CA 92093.

²Department of Biochemistry, University of Utah School of Medicine, Salt Lake City, UT 84112.

³ Laboratory for Immunochemical Circuits, La Jolla Institute for Immunology, La Jolla, CA 92037

⁴Skaggs School of Pharmacy and Pharmaceutical Sciences, University of California San Diego, La Jolla, CA 92093.

*These authors contributed equally.

#Correspondance: justin.english@biochem.utah.edu, fmferguson@ucsd.edu.

1 ABSTRACT

2 Unbiased chemical biology strategies for direct readout of protein interactome remodelling by
3 small molecules provide advantages over target-focused approaches, including the ability to
4 detect previously unknown targets, and the inclusion of chemical off-compete controls leading to
5 high-confidence identifications. We describe the BioTAC system, a small-molecule guided
6 proximity labelling platform, to rapidly identify both direct and complexed small molecule binding
7 proteins. The BioTAC system overcomes a limitation of current approaches, and supports
8 identification of both inhibitor bound and molecular glue bound complexes.

9

10 INTRODUCTION

11 Small molecule targeted therapies are a cornerstone of modern medicine, providing effective
12 treatments for a wide range of diseases. However, the clinical effects of candidate therapies in
13 patients can be highly variable, even when they bind the same therapeutic target with equal
14 affinity.¹ This divergent pharmacology may be due to uncharacterized off-target effects,
15 combinatorial polypharmacology, or from small molecules inducing changes in the interactome of
16 their protein targets through allosteric effects or ‘molecular glue’ effects.² Despite the critical role
17 of small molecules in drug discovery and development, there is a lack of comprehensive, network-
18 scale profiling methods that inform on the cellular interactomes of small molecules.

19 Examples of small-molecule mediated interactome rewiring are well studied in cancer, where
20 targeted therapies frequently induce functional changes in the complexation of their protein
21 targets. For example, blockbuster cancer drugs, such as trametinib¹ and lenalidomide³⁻⁵, exert
22 efficacy through the promotion of novel protein complexes, now known as ‘molecular glue’
23 pharmacology. Unanticipated protein complex rewiring is also a major cause of drug candidate
24 failures, for example underpinning adverse effects of 1st generation RAF inhibitors in RAS driven
25 tumors⁶, and resistance to BET bromodomain inhibitors in triple-negative breast cancer and
26 neuroblastoma^{7,8}. However, the discovery of interactome changes that mediate both drug efficacy
27 and drug resistance has so far been serendipitous, as researchers investigate why certain drugs
28 display unexpected pharmacology in the clinic. Despite their central importance, effects on target
29 complexation remain uncharacterized for most protein ligands, representing a ‘blind spot’ in
30 compound characterization workflows.

31 Current gold-standard technologies for unbiased target-ID are the chemical proteomic techniques
32 photoaffinity labelling⁹ and microenvironment mapping (μ Map)¹⁰ that use UV-light initiated
33 diazirine photochemistry to label liganded proteins with affinity handles. Here, off-compete
34 experiments with free drug, or comparison to a chemically matched negative control molecule
35 facilitate data interpretation. However, in the intracellular context these techniques are directed
36 towards detection of the primary target(s) only, due to the short half-life of the generated reactive
37 carbene species which corresponds to a labelling radius of ~ 6 nm. Here, the linker length
38 between the diazirine or iridium photocatalyst and the drug dictates the labelling radius, and is
39 therefore limited by cell permeability of the conjugate.¹⁰ As such, they have yet to be applied to
40 map drug-bound complexes. Diazirine photochemistry approaches are also currently
41 incompatible with *in vivo* applications.

42 To understand drug-induced interactome changes, affinity purification coupled to mass
43 spectrometry (AP/MS) and proximity labeling coupled to mass spectrometry are commonly
44 employed.¹¹ Proximity labeling techniques such as BiOID and Turboid are particularly

45 advantageous in mapping interactomes. Proximity labeling methods have a labeling radius of up
46 to 35 nm and can be used in live cells and animals.¹² By fusing a target protein or localization tag
47 with a proximity labeling enzyme proximity labeling can reliably detect transient, moderate affinity
48 protein-complex interaction *in situ* due to the ability of biotin ligase to accumulate affinity tags on
49 these protein partners over time.¹³ However, both techniques rely on *a priori* target knowledge,
50 which is often incompletely understood for drug candidates, and the fusion of the target protein to
51 either an affinity-tag or a proximity labeling enzyme, which can significantly impact interacting
52 proteins.¹³ Therefore, they cannot be used for unbiased interactome-ID of small molecules. The
53 outputs of these techniques are also typically large numbers of enriched proteins, due to their low
54 stringency, making data interpretation and validation challenging.

55 To facilitate routine evaluation of ligand-target interactome changes induced by either inhibitors
56 or molecular glues in a single experiment, we envisioned a method that combines the precision
57 and unbiased nature of chemical proteomics with the sensitivity, whole-organism compatibility,
58 and extended detection radius of proximity-labelling coupled to mass spectrometry. Here, we
59 report the development of a ligand-guided miniTurbold method to accomplish these goals, and
60 benchmark it against gold-standard unbiased technologies for both target-ID and interactome-ID.

61

62 RESULTS

63 Our method, named the biotin targeting chimera (BioTAC) system, uses bifunctional molecules
64 composed of a compound-of-interest linked to selective FKBP12^{F36V} recruiter orthoAP1867, to
65 recruit a ligandable proximity labeling enzyme (mTurbo-FKBP12^{F36V}) to compound-bound
66 complexes enabling their biotinylation and subsequent affinity purification (Figure 1a-b). To
67 benchmark the BioTAC system for accurate detection of the direct targets of ligands we selected
68 the well-characterized BET protein inhibitor (+)-JQ1, which potently binds BRD2, BRD3 and
69 BRD4 (as well as the testes-specific BET protein BRDT), as a test case.¹⁴ We synthesized a
70 series of bifunctional molecules consisting of (+)-JQ1 conjugated to orthoAP1687 via a variable

71 linker (Figure 1b, Figure S1a-c). We measured (+)-JQ1-bifunctional molecule cell permeability
72 using an FKBP12^{F36V} cellular target engagement assay adapted from Nabet *et. al.* Briefly,
73 FKBP12^{F36V} binding molecules compete with an FKBP12^{F36V} targeting PROTAC (dTAC-13), for
74 NLuc-FKBP12^{F36V} occupancy, rescuing degradation and resulting in an increase in NLuc/FLuc
75 (control) signal relative to DMSO-treated cells.¹⁵ All synthesized compounds were comparably
76 cell permeable (Figure S1d-e)¹⁵.

77 We next performed bifunctional molecule guided-proximity labeling experiments using our
78 validated reagents. HEK293 cells transiently transfected with mTurbo-FKBP12^{F36V} were treated
79 with 100 μ M biotin, 1 μ M bifunctional (+)-JQ1 recruiters, and variable concentrations of free (+)-
80 JQ1 to off-compete the bifunctional molecule and rescue biotinylation. Biotinylated proteins were
81 isolated from cell lysates via streptavidin bead pulldown and analyzed by western blot for BRD4,
82 a primary target of (+)-JQ1. We observed significant enrichment of BRD4 and a dose dependent
83 decrease in BRD4 pulldown in the presence of unconjugated (+)-JQ1 at all timepoints evaluated
84 (Figure 1c, Figure S1g-j). Comparable activity was observed for all bifunctional analogues,
85 indicating low sensitivity to linker length (Figure S1g-j), FMF-01-147-1 (Cpd 1) was selected for
86 further characterization based on high BRD4-labeling and rescue at the 30 min time point (Fig.
87 1c).

88 Having determined that the BioTAC system could identify BRD4 as a (+)-JQ1 target in focused
89 screens, we sought to evaluate it as an unbiased target-ID method. To identify direct binders of
90 (+)-JQ1 proteome-wide, we performed BioTAC proximity labelling experiments as described
91 above, followed by label-free mass spectrometry-based proteomic analysis of biotinylated
92 proteins enriched following a 30 minute treatment with 100 μ M biotin plus DMSO or 1 μ M Cpd 1,
93 and then 1 μ M Cpd 1 off-competed by pre-treatment with 10 μ M free (+)-JQ1. We observed highly
94 selective enrichment of known (+)-JQ1 targets BRD3 and BRD4, comparable to published (+)-
95 JQ1 μ Mapping and superior to published (+)-JQ1 photoaffinity labelling (Figure 1d-e, Figure S2a-
96 c, Figure S3a-c, Table S1).

97 Having established conditions for determining the primary targets of small molecules using the
98 BioTAC system, we next investigated its utility in reading out the interactome sphere of (+)-JQ1
99 bound BET-proteins. An advantage of the BioTAC system is the relatively long half-life of the
100 activated biotin-AMP intermediate generated by TurboID, allowing the labelling radius to be
101 increased up to 35 nm by extending the labelling time.¹² To quantitively evaluate the ability of the
102 BioTAC system to successfully enrich the known interactome of (+)-JQ1 bound BET proteins, we
103 performed time course BioTAC proximity labelling experiments at the 1 h and 4 h time points, and
104 evaluated streptavidin-enriched biotinylated proteins using mass spectrometry-based proteomic
105 analysis ([Figure 2a-c](#), [Figure S3](#), [Table S1](#)). As expected, longer time points correlated with a
106 greater number of proteins meeting our significance cut-offs (defined as $FC > 2$, $P < 0.05$) for both
107 enrichment in Cpd 1 vs. DMSO, and competition with free (+)-JQ1 in Cpd 1 vs. Cpd 1 + 10 μ M
108 (+)-JQ1, ([Figure 2a](#), [Figure S3](#)). Known (+)-JQ1 direct targets BRD3 and BRD4 were significantly
109 enriched and off-competed at all time points and BRD2 was also detected at the 4 hr timepoint.
110 Encouragingly, identified hit proteins at 1-4 hrs also included many known BET interactors, such
111 as proteins found in components of the Pol II productive elongation complex subunit P-TEFb, the
112 TFIID complex, and the Nucleosome Remodeling Deacetylase (NuRD) complex, as well as
113 known BRD4 direct-binder Histone H4 ([Table S1](#)). These observations suggested that we may
114 be labelling direct interactors of (+)-JQ1 bound BRD2, 3, and 4. To test this hypothesis we
115 compared our hits to an extensive BET protein interactome reference dataset identified using
116 AP/MS and proximity labelling coupled to mass spectrometry with and without (+)-JQ1, reported
117 by Lambert *et al.*¹⁶ The BioTAC system afforded significant enrichment and off-competition ($P <$
118 0.0001, one-way ANOVA) of identified reference interactors at the 4 h time point ([Figure 2b](#)). We
119 next asked whether we could perform the inverse, enriching complex members identified by
120 Lambert *et al.* directly from our data without any *a priori* knowledge of known interactors. We were
121 pleased to discover that 60% of our statistically significant enriched and (+)-JQ1 rescued hits were
122 also present in the Lambert dataset. This observation falls greater than 7 standard deviations

123 above a random bootstrap analysis of our data without filtering for significant enrichment and (+)-
124 JQ1 rescue (Figure 2c). To account for the limitations of using the findings of only one study as a
125 benchmark, we performed Gene Ontology (GO) Biological Process analysis of the hits from the
126 4hr timepoint^{17,18}. Here, transcriptional elongation by Pol II was significantly enriched ($P < 0.05$),
127 consistent with the known functions of BET protein containing complexes targeted by
128 bromodomain inhibitors (Figure 2d).¹⁹

129 The paucity of practical methods for rapid, unbiased readout of small-molecule induced
130 interactome changes has hindered the rational discovery and development of molecular glues.
131 Molecular glues are small molecules which exert their function by binding a primary target, and
132 promoting or strengthening its interaction with a second protein through interactions at the protein-
133 protein interface.²⁰ Molecular glue discovery is an area of high biomedical interest due to the
134 ability of molecular glues to target undruggable oncoproteins such as transcription factors, which
135 are recalcitrant to traditional inhibitor discovery but can be neutralized by induced complexation
136 and targeted degradation.²⁰ However, as the binary affinity between a molecular glue and the
137 second recruited target is low or non-existent in the absence of the primary target, molecular glue
138 interactions are challenging to detect and screen for. Having rigorously benchmarked the
139 performance of the BioTAC system using well-characterized (+)-JQ1, we sought to use the
140 BioTAC system to inform on complexes assembled by molecular glues (Figure 3a).²⁰ We selected
141 Trametinib as a non-dergrader glue with which to benchmark the platform. Trametinib derives its
142 clinical anti-cancer efficacy from promoting the interaction of its primary target MEK1/2 with KSR1,
143 but has low affinity for KSR1 alone meaning this interaction was missed during clinical
144 developments.¹

145 We synthesized bifunctional trametinib analogue JWJ-01-280/Cpd 2, with a linker attachment
146 informed by a reported trametinib-derived BODIPY-linked BRET probe named Tram-bo (Figure
147 3b).¹ We evaluated the cell permeability of Cpd 2 as described above, which was less cell
148 permeable than the (+)-JQ1 derivatives (Figure S4a). Nevertheless, Cpd 2 supported efficient

149 MEK1 labelling, following dose and time point optimization (Figure S4b-c). We evaluated the
150 ability of the BioTAC system to detect both known interactors of trametinib by Western blot, as
151 described above. We successfully detected the MEK1:trametinib:KSR1 complex using the
152 BioTAC system following a 4 hr treatment with 1 μ M Cpd 2, and dose-dependent competition in
153 the presence of trametinib of both KSR1 and MEK1 by immunoblot (Figure 3c, Figure S6). Low
154 expression of KSR1 in HEK293 cells resulted in lower KSR1 signal relative to MEK1 in both input
155 and enriched samples, indicating that a small proportion of MEK1 in HEK293s is bound by KSR1
156 in the presence of trametinib. In line with the reported finding that trametinib binds more tightly,
157 and with a slower off-rate (K_{dis}) to MEK1-KSR1 than to MEK1 alone, higher concentrations of
158 trametinib were required to off-compete labelling of KSR1 than MEK1.¹ To strengthen our
159 confidence that the MEK1: trametinib: KSR1 complex can be reliably detected by BioTAC, and to
160 allow quantification of enrichment and competition, we turned to published conditions from Khan
161 *et al.*¹ We repeated the BioTAC experiment, this time with mKSR1 overexpressed concomitantly
162 with mTurbo-FKBP12^{F36V}, and observed significant enrichment of KSR1 in the presence of Cpd 2
163 and convincing off-competition by trametinib (Figure 3d, Figure S6). To examine the global
164 interactome of Trametinib in cells, we performed BioTAC experiments with Cpd 2, coupled to
165 mass spectrometry. Here, we successfully enriched KSR1, alongside other known MEK1/2
166 interactors AFAR and BRAF (Figure 3e). Together, these data demonstrate the ability of the
167 BioTAC system to detect the complexes assembled by non-degrader molecular glues.
168

169 **DISCUSSION**

170 Methods for the routine measurement of drug-target interactomes are lacking, hiding the
171 mechanism of action of numerous small molecules from view. Even though interactome
172 remodelling in response to small molecule drugs is a common phenomenon that mediates drug
173 efficacy and resistance, little progress has been made in identifying and characterizing such
174 events. Here we report the BioTAC system, which can identify the direct target of a small

175 molecule, as well as its complexed proteins with high confidence. We demonstrate successful
176 enrichment of the reported interactomes of the epigenetic inhibitor (+)-JQ1 and the molecular glue
177 trametinib, but this approach is theoretically applicable to any small molecule of interest that can
178 be functionalized with a linker.

179 Next, we show the BioTAC system can identify molecular glue pairs that previously evaded
180 detection, in a single experiment using trametinib, MEK1/2, KSR1, as a model system. The
181 discovery and detection of molecular glue interactions is notoriously challenging to evaluate, in
182 particular when evaluating non-degrader molecular glues. Recently, elegant workflows consisting
183 of mechanism-based screening in wild-type and hypo-NEDDylated cells, followed by multi-omic
184 target deconvolution have been described for the discovery of cullin-ring ligase (CRL)-recruiting
185 molecular glue degraders.^{21,22} To identify non-degrader molecular glues, size exclusion
186 chromatography coupled to mass spectrometry has been used in combination with activity-based
187 protein profiling to screen electrophilic compound libraries, yielding covalent stabilizers and
188 disruptors of protein-protein interactions.²³ However, these approaches require resource intensive
189 multi-omic workflows, and are limited to covalent glues, or CRL-mediated degradation
190 mechanisms. In future applications, we envision the BioTAC system may be used in a screening
191 mode, for unbiased profiling of putative glue libraries.

192 The BioTAC system uses a universal recruitable biotin ligase chimera, miniTurbo, facilitating rapid
193 application. Bifunctional molecules for investigating any drug-of-interest are synthesised in one
194 step from a common ortho-AP1867 precursor using robust coupling chemistries. Finally, the
195 enrichment, mass spectrometry and data analysis methods are adapted from standard protocols
196 in proximity labelling already performed by most proteomics core facilities.²⁴ These features make
197 BioTAC system readily accessible for broad application. During the preparation of this manuscript,
198 a preprint describing a related approach for identifying targets of small molecules via SNAP- and
199 Halo-tagging of TurboID was also disclosed.²⁵ Whilst these systems differ from the BioTAC
200 system in their reported specificity, and have not yet been benchmarked for interactome-

201 detection, their successful implementation across a range of ligands highlights the robustness of
202 using proximity labelling to interrogate small molecule targets.²⁵
203 In the long term, building community-wide knowledge around how small molecule drugs alter their
204 target proteins complexation will lay the foundation for the rational design of drug target
205 interactome profiles, to combat drug resistance, and enable wider targeting of the undruggable
206 proteome.

207

208 **AUTHOR CONTRIBUTIONS**

209 F.M.F. and J.G.E. conceived and led the study. J.G.E. designed and cloned the DNA constructs.
210 J.W.J. and F.M.F. designed and performed molecule synthesis. A.J.T. and G.E.G. performed dual
211 luciferase target engagement assays. A.J.T. and B.T.B. performed immunoblot experiments.
212 A.J.T. prepared samples for proteomic studies. A.J.T., S.A.M. and J.G.E. performed proteomic
213 data analysis. F.M.F. wrote the manuscript with input from all authors.

214

215 **ACKNOWLEDGEMENTS**

216 This work was supported by American Cancer Society IRG Grant # IRG-19-230-48-IRG, UC San
217 Diego Moores Cancer Center, Specialized Cancer Center Support Grant NIH/NCI P30CA023100,
218 and NIH grant DP2NS132610 (F.M.F.). A.J.T. was supported by a UCSD Distinguished Graduate
219 Student Award. G.E.G. was supported by the Molecular Biophysics Training Grant T32
220 32GM139795. This study was supported by NIH grant DP2GM146247 (J.G.E.). The authors
221 would like to thank Dr. Majid Ghassemian, Dr. Lisa Jones, and Dr. Katherine A. Donovan for
222 helpful discussions and feedback and Dr. Sonya Neal for use of a BioRad ChemiDoc Gel Imager.

223

224 **DISCLOSURES**

225 AJT, JJ, JGE and FMF are inventors on a patent relating to this work jointly owned by the
226 University of California San Diego, Dana-Farber Cancer Institute and University of Utah. FMF is

227 a scientific co-founder and equity holder in Proximity Therapeutics, a scientific advisory board
228 member (SAB) and equity holder in Triana Biomedicines. Fleur Ferguson is or was recently a
229 consultant or received speaking honoraria from Eli Lilly and Co., RA Capital, Tocris BioTechne,
230 and Plexium Inc. The Ferguson lab receives or has received research funding from Ono
231 Pharmaceutical Co. Ltd and Merck & Co. JGE is a scientific co-founder, equity holder, and
232 scientific advisory board (SAB) member in Evolution Bio. The English lab receives or has received
233 research funding from Eli Lilly.
234
235

236 **REFERENCES**

237 1 Khan, Z. M. *et al.* Structural basis for the action of the drug trametinib at KSR-bound MEK.
238 *Nature* **588**, 509-514 (2020). <https://doi.org/10.1038/s41586-020-2760-4>

239 2 Ferguson, F. M. & Gray, N. S. Kinase inhibitors: the road ahead. *Nat Rev Drug Discov* **17**,
240 353-377 (2018). <https://doi.org/10.1038/nrd.2018.21>

241 3 Ito, T. *et al.* Identification of a primary target of thalidomide teratogenicity. *Science* **327**,
242 1345-1350 (2010). <https://doi.org/10.1126/science.1177319>

243 4 Kronke, J. *et al.* Lenalidomide causes selective degradation of IKZF1 and IKZF3 in
244 multiple myeloma cells. *Science* **343**, 301-305 (2014).
<https://doi.org/10.1126/science.1244851>

245 5 Lu, G. *et al.* The myeloma drug lenalidomide promotes the cereblon-dependent
246 destruction of Ikaros proteins. *Science* **343**, 305-309 (2014).
<https://doi.org/10.1126/science.1244917>

247 6 Holderfield, M., Nagel, T. E. & Stuart, D. D. Mechanism and consequences of RAF kinase
248 activation by small-molecule inhibitors. *Br J Cancer* **111**, 640-645 (2014).
<https://doi.org/10.1038/bjc.2014.139>

249 7 Shu, S. *et al.* Response and resistance to BET bromodomain inhibitors in triple-negative
250 breast cancer. *Nature* **529**, 413-417 (2016). <https://doi.org/10.1038/nature16508>

251 8 Iniguez, A. B. *et al.* Resistance to Epigenetic-Targeted Therapy Engenders Tumor Cell
252 Vulnerabilities Associated with Enhancer Remodeling. *Cancer Cell* **34**, 922-938 e927
253 (2018). <https://doi.org/10.1016/j.ccr.2018.11.005>

254 9 West, A. V. & Woo, C. M. Photoaffinity Labeling Chemistries Used to Map Biomolecular
255 Interactions. *Israel Journal of Chemistry*, e202200081 (2022).

256 10 Trowbridge, A. D. *et al.* Small molecule photocatalysis enables drug target identification
257 via energy transfer. *Proc Natl Acad Sci U S A* **119**, e2208077119 (2022).
<https://doi.org/10.1073/pnas.2208077119>

258 11 Richards, A. L., Eckhardt, M. & Krogan, N. J. Mass spectrometry-based protein-protein
259 interaction networks for the study of human diseases. *Mol Syst Biol* **17**, e8792 (2021).
<https://doi.org/10.1525/msb.20188792>

260 12 May, D. G., Scott, K. L., Campos, A. R. & Roux, K. J. Comparative Application of BioID
261 and TurboloID for Protein-Proximity Biotinylation. *Cells* **9** (2020).
<https://doi.org/10.3390/cells9051070>

262 13 Qin, W., Cho, K. F., Cavanagh, P. E. & Ting, A. Y. Deciphering molecular interactions by
263 proximity labeling. *Nat Methods* **18**, 133-143 (2021). <https://doi.org/10.1038/s41592-020-01010-5>

264 14 Filippakopoulos, P. *et al.* Selective inhibition of BET bromodomains. *Nature* **468**, 1067-
265 1073 (2010). <https://doi.org/10.1038/nature09504>

266 15 Nabet, B. *et al.* Rapid and direct control of target protein levels with VHL-recruiting dTAG
267 molecules. *Nat Commun* **11**, 4687 (2020). <https://doi.org/10.1038/s41467-020-18377-w>

268 16 Lambert, J. P. *et al.* Interactome Rewiring Following Pharmacological Targeting of BET
269 Bromodomains. *Mol Cell* **73**, 621-638 e617 (2019).
<https://doi.org/10.1016/j.molcel.2018.11.006>

270 17 Ashburner, M. *et al.* Gene ontology: tool for the unification of biology. The Gene Ontology
271 Consortium. *Nat Genet* **25**, 25-29 (2000). <https://doi.org/10.1038/75556>

272 18 Gene Ontology, C. The Gene Ontology resource: enriching a GOld mine. *Nucleic Acids
273 Res* **49**, D325-D334 (2021). <https://doi.org/10.1093/nar/gkaa1113>

274 19 Schwalm, M. P. & Knapp, S. BET bromodomain inhibitors. *Curr Opin Chem Biol* **68**,
275 102148 (2022). <https://doi.org/10.1016/j.cbpa.2022.102148>

284 20 Domostegui, A., Nieto-Barrado, L., Perez-Lopez, C. & Mayor-Ruiz, C. Chasing molecular
285 glue degraders: screening approaches. *Chem Soc Rev* **51**, 5498-5517 (2022).
286 <https://doi.org/10.1039/d2cs00197g>

287 21 Mayor-Ruiz, C. et al. Publisher Correction: Rational discovery of molecular glue degraders
288 via scalable chemical profiling. *Nat Chem Biol* **17**, 361 (2021).
289 <https://doi.org/10.1038/s41589-021-00735-4>

290 22 King, E. A. et al. Chemoproteomics-Enabled Discovery of a Covalent Molecular Glue
291 Degrader Targeting NF- κ B. *bioRxiv*, 2022.2005.2018.492542 (2022).
292 <https://doi.org/10.1101/2022.05.18.492542>

293 23 Lazear, M. R. et al. Proteomic discovery of chemical probes that perturb protein
294 complexes in human cells. *bioRxiv*, 2022.2012.2012.520090 (2022).
295 <https://doi.org/10.1101/2022.12.12.520090>

296 24 Cho, K. F. et al. Proximity labeling in mammalian cells with TurboID and split-TurboID. *Nat
297 Protoc* **15**, 3971-3999 (2020). <https://doi.org/10.1038/s41596-020-0399-0>

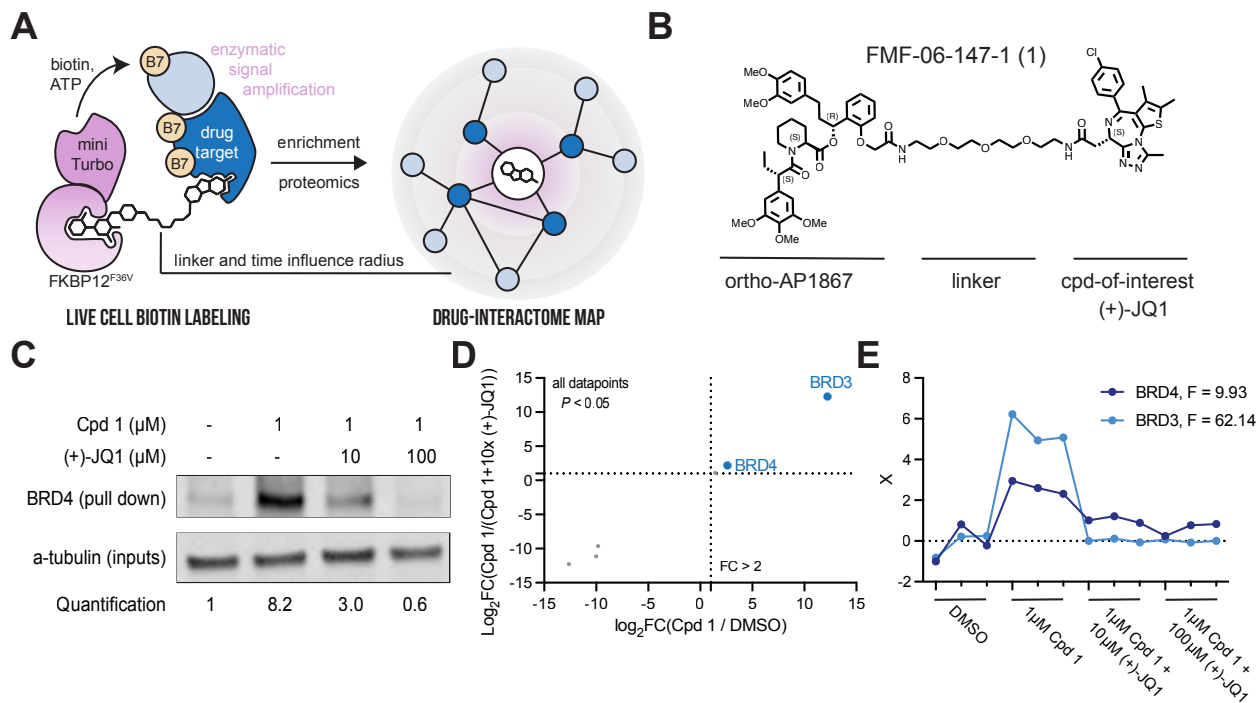
298 25 Venable, J. D. et al. Drug interaction mapping with proximity dependent enzyme recruiting
299 chimeras. *bioRxiv*, 2022.2009.2026.509259 (2022).
300 <https://doi.org/10.1101/2022.09.26.509259>

301 26 Gerhard, D. S. et al. The status, quality, and expansion of the NIH full-length cDNA project:
302 the Mammalian Gene Collection (MGC). *Genome Res* **14**, 2121-2127 (2004).
303 <https://doi.org/10.1101/gr.2596504>

304

305

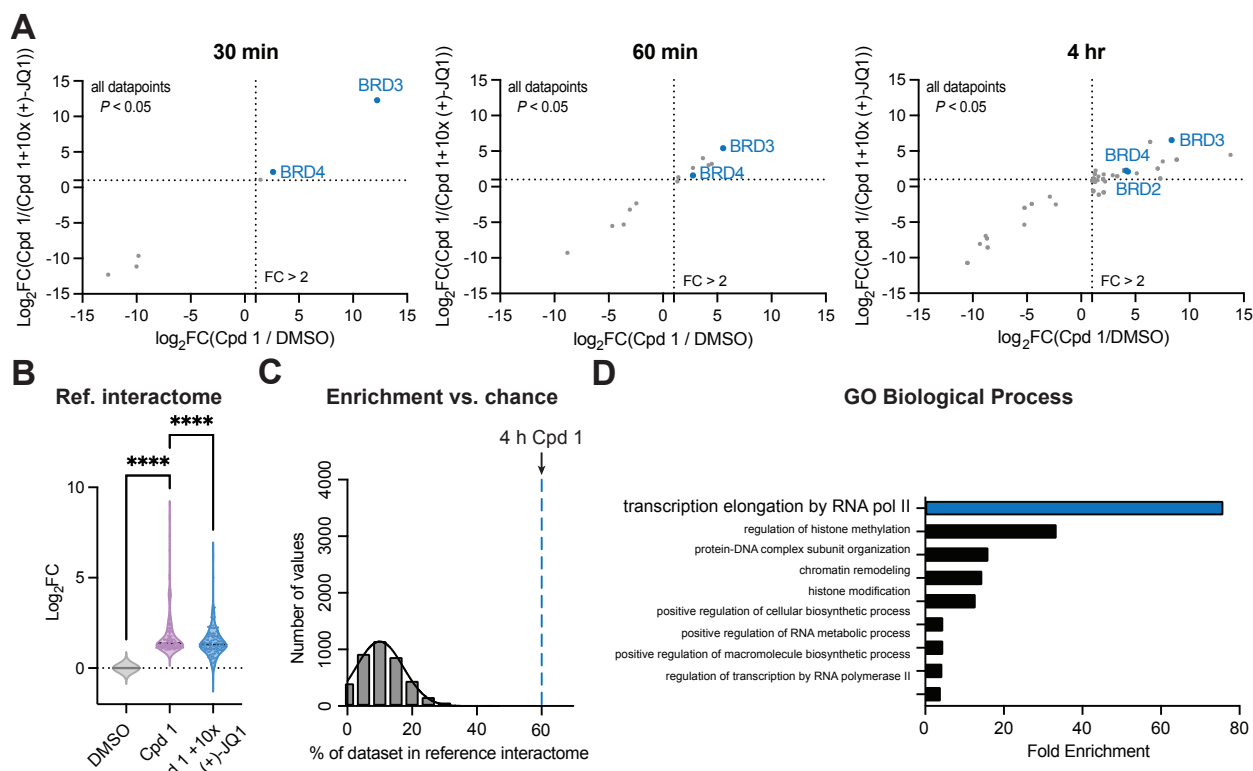
306 **FIGURES**



307

308 **Figure 1 | The BioTAC system enables rapid, accurate small molecule target-ID. A.**
309 Schematic depicting the components of the BioTAC system. B. Example molecule, Cpd 1,
310 annotated with key functional groups. C. Immunoblot analysis of BRD4 enrichment following
311 treatment of HEK293 cells transiently transfected with miniTurboFKBP12^{F36V} with the indicated
312 compounds and 100 μ M biotin at the 30 min timepoint. Data representative of $n = 2$ biologically
313 independent experiments (SI Figure 1J). D. Scatterplot displaying relative FC of streptavidin-
314 enriched protein abundance following treatment of HEK293 cells transiently transfected with
315 miniTurboFKBP12^{F36V} with the indicated compounds and 100 μ M biotin at the 30 min timepoint.
316 Only proteins with P -value < 0.05 in both conditions depicted. Complete datasets in Table S1,
317 plotted individually Figure S3. E. F-test analysis of proteomic data depicted in D., showing
318 significant enrichment of BRD3 and BRD4 in the presence of 1 μ M Cpd 1, relative to DMSO and
319 (+)-JQ1 off-compete experiments. F-statistic listed top right, X = scaled abundance ratio.

320

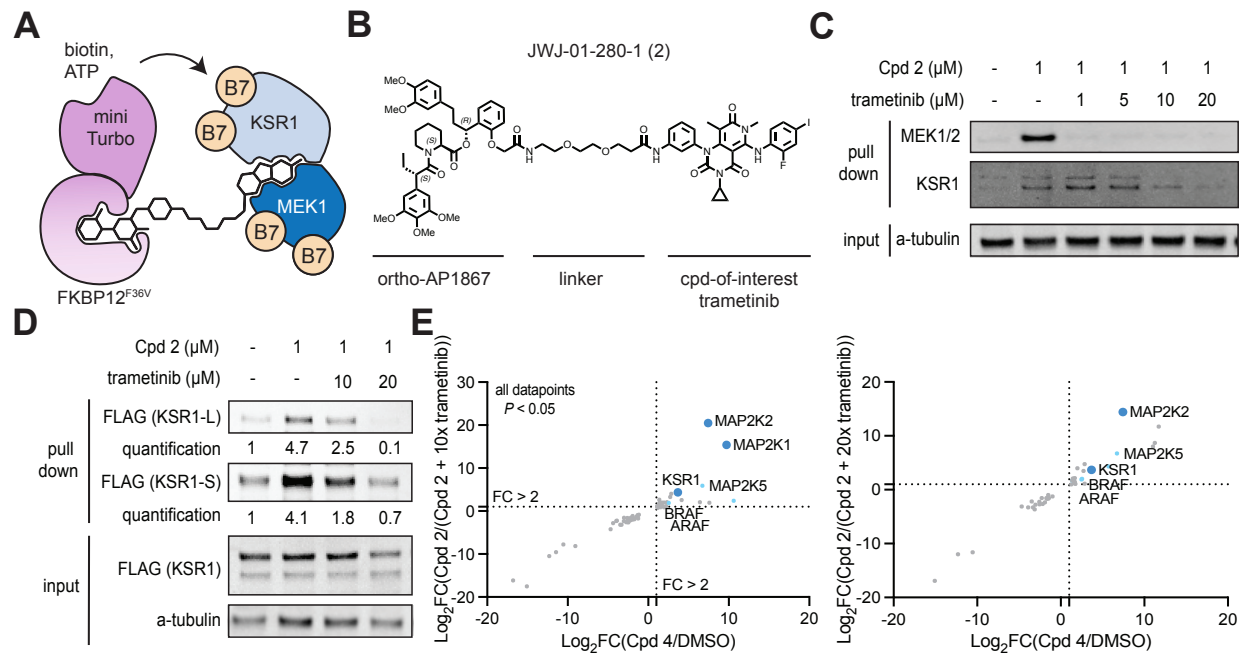


321

322 **Figure 2 | The BioTAC system enables rapid, accurate small molecule interactome-ID. A.**
323 Time-course proteomics of streptavidin-enriched biotinylated proteins isolated from HEK293 cells
324 transiently transfected with miniTurboFKBP12^{F36V} and treated with the indicated compounds and
325 100 μ M biotin, demonstrating enrichment and competition of known direct targets (30 min) and
326 complexed proteins (60 min, 4 hrs). Only proteins with P -value < 0.05 in both conditions depicted.
327 Complete datasets in Table S1, plotted individually Figure S3. High-confidence hits are defined
328 as those that are enriched > 2 -fold in both Cpd 1/ DMSO and Cpd 1 / Cpd 1 + 10x (+)-JQ1, where
329 $P < 0.05$, plotted upper-right quadrant. B. Fold-change of all reference BRD2, BRD3, and BRD4
330 interactors (Lambert *et. al.*) enriched in the Cpd 1 vs. DMSO dataset at the 4 hr time point,
331 showing statistically significant rescue ($P < 0.0001$, 1-way ANOVA). C. Percent enrichment of
332 reference interactors (Lambert *et. al.*) in the hits identified at the 4 hr timepoint (dotted line), vs.
333 the percent enrichment of known interactors in 4,000 random protein sets of equivalent size from
334 the DMSO control (gray bars), showing significant enrichment by Cpd 1 BioTAC (> 7 standard

335 deviations away from mean of random chance). D. Gene Ontology analysis, showing significant
336 enrichment of biological processes associated with known BET-protein function in the 4 hr Cpd 1
337 BioTAC experiment hits.

338



339

340 **Figure 3 | The BioTAC system enables detection of non-degrader molecular glue**
 341 **interactions.** A. Schematic depicting how the BioTAC system can detect molecular glue
 342 interactions. B. Chemical structure of Trametinib recruiting bifunctional molecule JWJ-01-280-
 343 1/Cpd 2. C. Immunoblot analysis of MEK1 and KSR1 following treatment of HEK293 cells
 344 transiently transfected with miniTurboFKBP12^{F36V} with the indicated compounds and 100 μM
 345 biotin at the 4 h timepoint, and streptavidin-based enrichment, showing successful enrichment
 346 and competition with trametinib. D. Immunoblot analysis of mKSR1 following treatment of HEK293
 347 cells transiently transfected with miniTurbo-FKBP12^{F36V} and mKSR1, with the indicated
 348 compounds and 100 μM biotin at the 4 h timepoint, and streptavidin-based enrichment, showing
 349 successful enrichment and competition with trametinib. In C, D two KSR1 isoforms are observed,
 350 produced by alternative splicing.²⁶ KSR1-L (102 KDa) corresponds to the expected MW of Uniprot
 351 Q8IVT5-1 (canonical sequence), KSR1-S (87 KDa) corresponds to the expected MW of variant
 352 with residues 1-137 missing, Uniprot Q8IVT5-3, and -4. Our data indicate both isoforms can
 353 complex with trametinib-bound MEK1.